CRYSTAL DISSOLUTION AND PRECIPITATION IN POROUS MEDIA FLOW: VARIABLE GEOMETRY

T.L. VAN NOORDEN AND I.S. POP AND C.J. VAN DUIJN[1]

[1] Department of Mathematics and Computer Science, Technische Universiteit Eindhoven, PO Box 513, 5600 MB Eindhoven, The Netherlands

Abstract

We consider a porous medium that is fully saturated by a fluid in which cations and anions are dissolved. In a precipitation reaction, the cations and anions can precipitate in the form of crystalline solid, attached to the surface of the grains (the porous matrix). The reverse reaction of dissolution is also possible. For describing the dissolution and precipitation reaction, we use the model from Knabner et al. [2] and Van Duijn et al. [5]. In these works no changes in the flow domain are taken into account. Here we allow changes in the flow domain as a result of the precipitation and dissolution of crystals. For simple geometries we show that solutions to the model equations exist and we study their qualitative behavior using both analytic and numerical techniques.

1. INTRODUCTION

In this paper we introduce and discuss a pore-scale model for crystal dissolution and precipitation. We consider a flow through a porous medium that is fully saturated. Ions dissolved in the fluid are transported by the flow. One could think of e.g. sodium (Na^+) and chlorine (Cl^-) ions. At the grain surface the dissolved ions can precipitate in the form of crystals that are attached to the grain. The reverse reaction of dissolution is also possible. Figure 1 presents a schematic representation of the situation.

Our investigations are a first step towards an upscaled model for crystal formation in reactive porous media flows and are motivated by the work of Knabner et al. [2] and Van Duijn et al. [5]. There the dissolution and precipitation of crystals do not affect the geometry of the problem. Here we pay special attention to the changes of geometry of the flow domain, which are due to the variation in thickness of the crystalline layer.

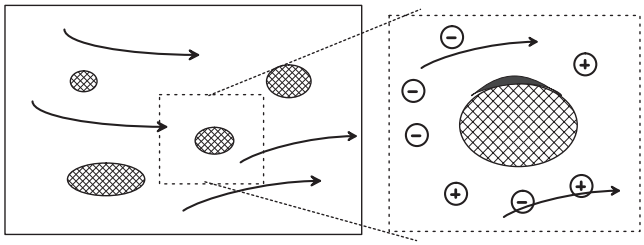

Figure 1. Schematic representation of the porous matrix. Crystals are attached to the grain surfaces, and cations and anions are dissolved in the fluid.

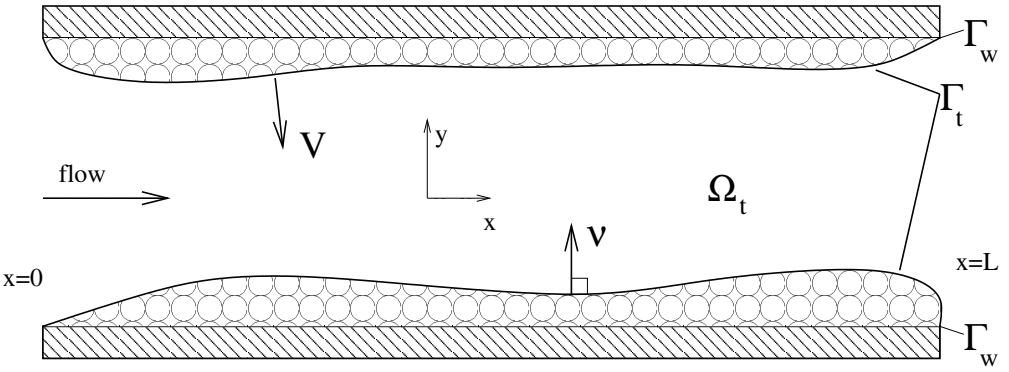

FIGURE 2. Schematic representation of the pore-scale geometry. The domain Ω_t is occupied by the fluid, and a layer of crystals is attached to the grain surface Γ_w.

2. THE MODEL

We consider the time dependent domain $\Omega_t \subset \mathbb{R}^d$, as shown in Fig. 2, which is the region in between the grains. Suppose Ω_t is occupied by a fluid in which cations (M_1) and anions (M_2) are dissolved. In a precipitation reaction n_1 particles of M_1, and n_2 particles of M_2 can precipitate in the form of one particle of a crystalline solid M_{12}, which is attached to the surface of the grains, denoted by Γ_w. The reverse reaction of dissolution is also possible:

$$M_{12} \leftrightarrows n_1 M_1 + n_2 M_2$$

The interface between the fluid phase and the crystalline solid is denoted by Γ_t

Denoting by c_i $(i = 1, 2)$ the molar concentration of the ions (mol/m^d), mass conservation gives the equations

$$\begin{aligned} \partial_t c_i + \nabla \cdot (q c_i - D \Delta c_i) &= 0 \quad \text{for} \quad x \in \Omega_t, \\ (n_i \rho - c_i) V &= D \nu \cdot \nabla c_i \quad \text{for} \quad x \in \Gamma_t. \end{aligned}$$

Here q (m/s) stand for the fluid velocity, ρ (mol/m^3) denotes the molar density of the crystalline solid, while V (m/s) denotes the growth speed of the layer of crystals in the normal direction ν. The diffusion constant is denoted by D (m^2/s).

At the location x on the variable surface Γ_t, the effect of dissolution and precipitation is described by the equation

$$\rho V = (r_p - r_d). \tag{1}$$

Here r_p (mol/s m^{d-1}) denotes the precipitation rate expressed by

$$r_p = k_p r(c_1, c_2),$$

with k_p (mol/s m^{d-1}) a positive rate constant and r a rate function depending on c_1 and c_2. A typical example, provided by mass action kinetics, is

$$r(c_1, c_2) = c_1^{n_1} c_2^{n_2}.$$

The dissolution rate $r_d = k_d$ (mol/s m^{d-1}) is constant (with $k_d > 0$) in the presence of crystals. Wherever there are crystals, the distance $d(x, \Gamma_w)$ from the location x on Γ_t to the grain surface Γ_w is strictly positive. Furthermore the dissolution rate has to be such

that in the absence of crystal ($d(x,\Gamma_w)=0$) and for a fluid that is undersaturated, i.e., $r(c_1,c_2)\le k_d/k_p$, the overall rate is zero. To achieve this, we introduce the set-valued expression

$$r_d \in k_d H(d(x,\Gamma_w)),$$

where H denotes the Heaviside graph,

$$H(u)=\begin{cases} 0, & \text{if } u<0,\\ [0,1], & \text{if } u=0,\\ 1, & \text{if } u>0.\end{cases}$$

If c_1 and c_2 are such that

$$r(c_1,c_2)>\frac{k_d}{k_p},$$

we have oversaturation and precipitation ($V>0$) will occur. If the concentrations c_1 and c_2 are below the solubility product, i.e.,

$$r(c_1,c_2)<\frac{k_d}{k_p},$$

while crystal is present, we have $V<0$ and dissolution occurs. If it also happens that $d(x,\Gamma_w)=0$, we set

$$r_d=\frac{k_p}{k_d}r(c_1,c_2),$$

implying $V=0$. Summarizing this discussion, we have for the normal speed V of the interface between the fluid and the crystalline solid the equation

$$\rho V \in k_d\left(\frac{k_p}{k_d}r(c_1,c_2)-H(d(x,\Gamma_w))\right).$$

3. ANALYSIS

For the mathematical analysis, we make a number of simplifiations: we assume that the concentration for the anions and cations is the same, with $n_1=n_2=1$, such that we may set $v:=c_1=c_2$. We also assume no flow, i.e., $q=0$, and we consider only the one dimensional situation. After non-dimensionalizing the equations, we obtain

$$\begin{cases} \partial_t v=\partial_{xx}v, & \text{for } x\in(0,h(t)),\\ \partial_x v=0, & \text{for } x=0,\\ \partial_x v=(\rho-v)h'(t), & \text{for } x=h(t),\\ h'(t)=k(w(t)-r(v)), & \text{for } x=h(t),\\ w(t)\in H(1-h(t)), & \end{cases}$$

where the dimensionless number k is usually referred to as the Damköhler number. For the reaction rate function $r(v)$ we assume that there is a unique value v^* of v such that $r(v^*)=1$, with $v^*<\rho$.

We may transform the equations (3) to equations on a fixed domain using the coordinate transform, as also used in [3],

$$y = \int_x^{h(t)} (\rho - v(z,t))\, dz, \quad \tau = t. \tag{2}$$

For $u(y,\tau) = v(x,t)$ we obtain the equations

$$\begin{cases} \partial_\tau f(u) = \partial_{yy} u, & \text{for } 0 < y < h_0, \\ \partial_y u = k(r(u) - w(t)), & \text{for } y = 0, \\ h'(t) = -k(r(u) - w(t)), & \text{for } y = 0, \\ w(t) \in H(1 - h(t)), & \\ \partial_y u = 0, & \text{for } y = h_0, \\ u(y,0) = u_0(y) = v_0(x), & \text{for } \tau = 0. \end{cases} \tag{3}$$

where $h_0 = \int_0^{h(0)} \rho - v_0(y) dy$, and where $f(u) = 1/(\rho - u)$. Using the boundary conditions, we can easily show that

$$h(t) = \int_0^{h_0} f(u) dy. \tag{4}$$

This equality allows us to write the system of equations in a form with non-local boundary conditions. We also regularize the equations by replacing the Heaviside graph by the Lipschitz approximation

$$H_\delta(u) := \begin{cases} 0 & \text{if } u < 0, \\ u/\delta & \text{if } u \in [0, \delta], \\ 1, & \text{if } u > \delta. \end{cases} \tag{5}$$

After substituting (4) and (5) in (3), we obtain

$$\begin{cases} \partial_\tau f(u) = \partial_{yy} u, & \text{for } 0 < y < h_0, \\ \partial_y u = k(r(u) - H_\delta(1 - \int_0^{h_0} f(u) dy)), & \text{for } y = 0, \\ \partial_y u = 0, & \text{for } y = h_0, \\ u(y,0) = u_0(y) = v_0(x), & \text{for } \tau = 0. \end{cases} \tag{6}$$

For the equations (6), we are able to show that solutions satisfy a maximum principle:

Lemma 1. *Let u be a classical solution of the regularized, transformed equations, then*

$$0 \le u(x,t) \le \max(M, u^*).$$

Furthermore we are able to show the following result.

Theorem 1. *There exists a unique classical solution of the regularized, transformed equations.*

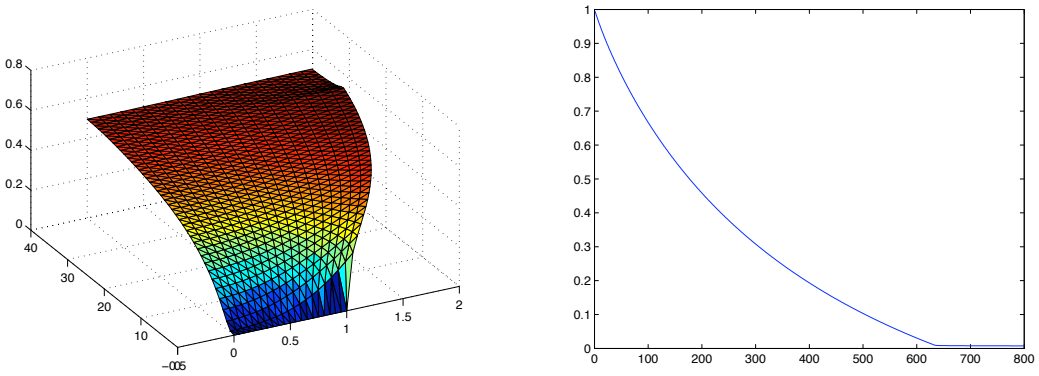

FIGURE 3. The ion concentration versus time and space (left), and the thickness of the crystal layer versus time (right).

4. SIMULATIONS

4.1. **Simulations: 1D.** In this section we present the results of some numerical computations of solutions of the model equations. We approximate solutions using the implicit Euler scheme, i.e., in each time step we solve the equations

$$\begin{cases} f(u(x,t_n)) = f(u(x,t_{n-1})) + \Delta t \partial_{xx} u(x,t_n), & \text{for } 0 < y < h_0, \\ \partial_x u(h_0,t_n) = 0, & \text{for } x = h_0, \\ \partial_x u(0,t) = -k(r(u(0,t_n) - H_\delta(1 - \int_0^{h_0} f(u(y,t_n))dy), & \text{for } x = 0, \end{cases}$$

These equations are discretized in the spatial variable x using finite differences. The integral is approximated using the trapezoidal rule. In this way we obtain a system of nonlinear equations that we solve using Newton's method.

The values for the parameters used in the numerical experiment are

$$\rho = 1, \quad L = 2, \quad h_1 = 1, \quad u_0 \equiv 0, \quad k = 1.$$

The nonlinear reaction rate is given by $r(u) = 3u^2$, and the regularization parameter δ for the Heaviside graph is set to 0.01. The interval $[0, h_1] = [0, 1]$ is divided in 100 subintervals, such that we obtain 101 equidistant nodes with $\Delta x = 0.01$. For Δt we take 0.005.

In order to be able to plot the solution v in the original coordinates, we need the inverse coordinate transform of (2), given by

$$x = \int_y^{h_1} f(u) d\bar{y}.$$

The approximate solution v is plotted in Figure 3, together with the thichness of the crystal layer.

4.2. **Simulations: 2D.** We consider a configuration as depicted in Figure 4: a square domain with in the lower left corner a grain in the form of a quarter circle. Initially there is a layer of crystals attached to the grain boundary. In the first part of the computations, the Dirichlet boundary at the top (see Fig. 4) is set to 0, and the layer of crystals will

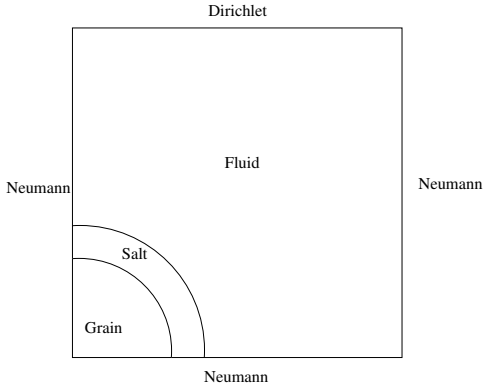

FIGURE 4. The 2D configuration; the crystals are occupying a banded region around the grain.

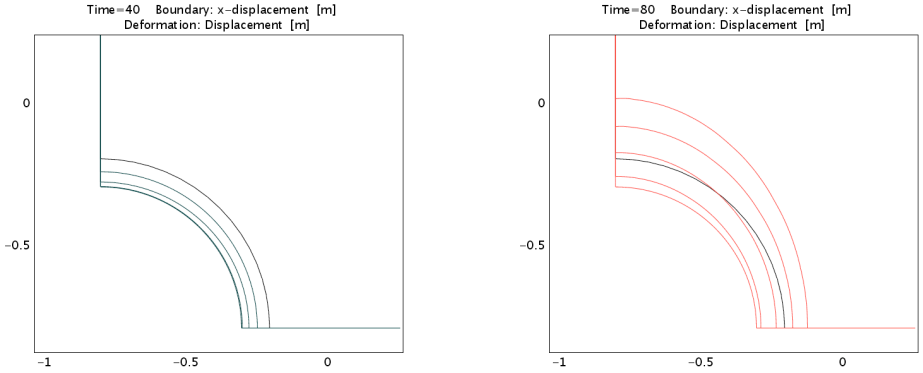

FIGURE 5. The layer of crystals in both in the dissolution (left) and precipitation (right) phases of the computation.

dissolve. The movement of the boundary of the layer in this phase of the computation is depicted in the left plot of Fig. 5. The position of the boundary is plotted each 10 time units. When $t = 40$, the Dirichlet boundary condition is set to 1. In this phase of the computations the layer of crystals will grow due to precipitation. Again, each 10 time units the position of the boundary is plotted in the right plot (together with the initial positions of the boundary).

In Figure 6, the cation concentration is given for $t = 80$. The left plot is the projection of the right plot onto the $z = 0$ plane, so that the change in the geometry can be clearly seen.

For the simulations, we use an ALE (arbitrary Lagrangian-Eulerian) [1] finite element method implemented in COMSOL. The method uses two reference frames (or coordinate systems), the spatial frame and the reference frame, see Fig. 7. The spatial frame is the usual, fixed coordinate system, with the spatial coordinates (x, y). In this coordinate system, the mesh moves. The reference frame is the coordinate system of the *reference coordinates* (X, Y). In this system, the mesh is fixed. In the left figure of Fig. 7 the initially undeformed mesh is shown. The spatial coordinate system (x, y) and the reference coordinate system (X, Y) coincide. In the right figure, the deformed mesh with coordinate

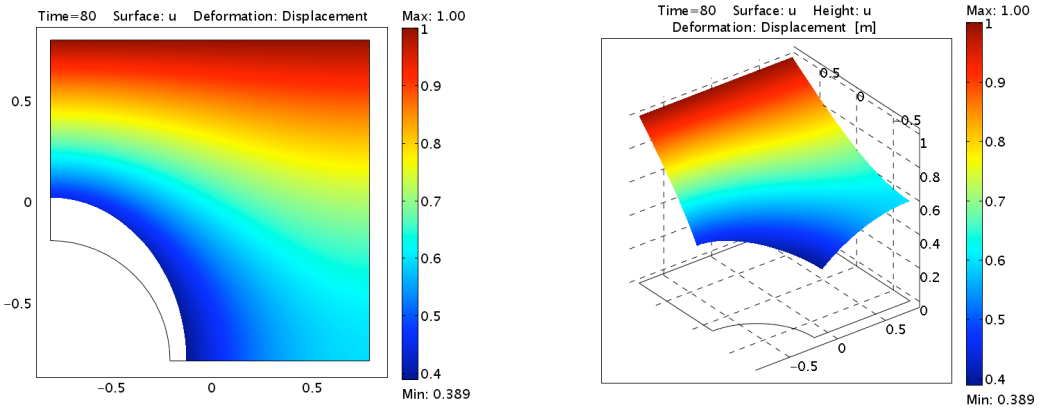

FIGURE 6. Cation concentration at the final time $t = 80$. The left plot is the projection of the right plot onto the $z = 0$ plane. Initially the fluid occupies the domain plotted in the $z = 0$ plane.

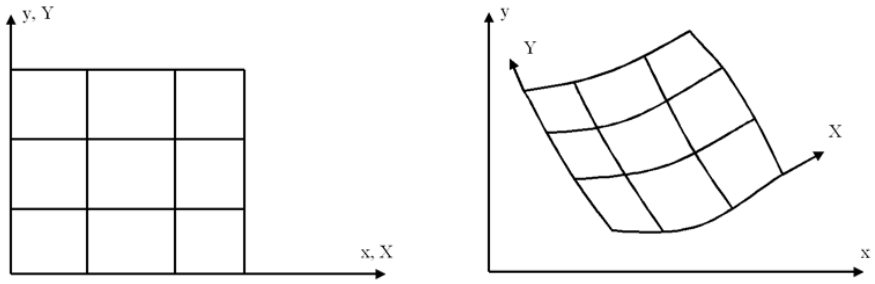

FIGURE 7. Initial (left) and deformed (right) mesh.

system (X, Y) is shown together with the fixed spatial coordinate system (x, y). The spatial and reference frames are related by the coordinate transformation

$$x = x(X, Y, t), \quad y = y(X, Y, t).$$

The velocity of the mesh nodes on the moving boundary is given by the equation (1) for the normal velocity V of the surface of the layer of crystals. The velocity of interior mesh nodes is given by the solution of the equations

$$\frac{\partial^2}{\partial X^2}\frac{\partial x}{\partial t} + \frac{\partial^2}{\partial Y^2}\frac{\partial x}{\partial t} = 0, \quad \frac{\partial^2}{\partial X^2}\frac{\partial y}{\partial t} + \frac{\partial^2}{\partial Y^2}\frac{\partial y}{\partial t} = 0.$$

5. CONCLUSIONS

In this paper, we have proposed a pore-scale model for crystal precipitation and dissolution. The model takes into account the changes in the geometry of the flow domain due to variations in the crystal layers attached to the boundary of the porous matrix. For the 1D cases we show existence and uniqueness of solutions, and we have developed simulation tools for the 1D and 2D cases.

Ongoing research focusses on analytical results for the 2D/3D cases, and on the upscaling of the model using (numerical) homogenization techniques.

References

1. Hirt, C., A. Amsden, and J. Cook (1974), An Arbitrary Lagrangian-Eulerian computing method for all flow speeds, *J. Comp. Phys., 14*, 227-253, reprinted in *135* (1997), 203-216.
2. Knabner, P., C.J. van Duijn and, S. Hengst, (1995), An analysis of crystal dissolution fronts in flows though porous media. Part I: Compatible boundary conditions, *Adv. Water Res., 18*, 171–185.
3. van de Fliert, B. W., and R. van der Hout, (2000), A generalized Stefan problem in a diffusion model with evaporation, *SIAM J. Appl. Math., 60*, 1128–1136.
4. van Duijn, C.J., P. Knabner, and R.J. Schotting, (1998), An analysis of crystal dissolution fronts in flows though porous media. Part II: Incompatible boundary conditions, *Adv. Water Res., 22*, 1–16.
5. van Duijn, C.J., and I.S. Pop, (2004), Crystal dissolution and precipitation in porous media: pore scale analysis, *J. reine angew. Math., 577*, 171–211.